

Vascular Remodelling is Impaired in Parkinson Disease

Panzao Yang^{1,3}, Henry Waldvogel^{2,4}, Clinton Turner^{2,5}, Richard Faull^{2,4}, Mike Dragunow^{1,2} and Jian Guan^{1,2*}

¹Department of Pharmacology and Clinical Pharmacology, Faculty of Medical and Health Sciences, University of Auckland, New Zealand

²Centre for Brain Research, Faculty of Medical and Health Sciences, University of Auckland, New Zealand

³Liggins Institute, University of Auckland, New Zealand

⁴Department of Anatomy and Medical Imaging, Faculty of Medical and Health Sciences, University of Auckland, New Zealand

⁵Department of Anatomical Pathology, LabPlus, Auckland City Hospital Auckland, New Zealand

Abstract

Objective: We have previously reported vascular degeneration of human Parkinson disease (PD). In which we described degenerative pathology of endothelial cells and its association with increased string vessels in the grey matter of middle frontal gyrus (MFG). Growth factors, for example platelet-derived growth factor (PDGF), insulin-like growth factor-1 (IGF-1) and vascular endothelial growth factor (VEGF), involve in vascular remodelling by promoting cell proliferations and angiogenesis through capillary pericytes. Thus current study examined the hypothesis whether vascular degeneration in human PD is associated with impairment of vascular remodelling.

Methods: Using tissue microarray method we conducted immuno histochemical staining in the grey matter of MFG of human PD (n=17) and age-matched control cases (n=17). The expression of PDGF receptor-beta, proliferating cell nuclear antigen and phosphorylation of IGF-1 receptor in capillaries, IGF binding protein-2 and VEGF were evaluated using automated image analysis software.

Results: PDGF receptor-beta was specifically expressed in the pericytes which formed capillary morphology. Compared to the age-matched control cases, there were significant decrease in PDGF receptor-beta positive capillaries ($p<0.05$; $p<0.01$), proliferating vascular cells ($p<0.05$) and VEGF ($p<0.05$) in the PD cases. There no difference in phosphorylation of IGF-1 receptors, expressed in the capillaries between the groups. We found a significant increase in IGF binding protein-2, expressed in the astrocytes of PD when compared to the control cases ($p<0.05$). Interestingly the levels of phosphorylated IGF receptors in the capillaries were significantly correlated with the numbers of pericytes and proliferating cells in capillaries ($p=0.001$).

Conclusion: Impaired PDGF function in the pericytes, reduced cell proliferation and VEGF suggested that the ability of vascular remodelling is impaired in PD. The maintained IGF-1 function appeared to be ineffective to retain vascular remodelling process in PD. The up-regulation of IGF binding protein-2 may suggest a role for autocrine/paracrine of IGF-1 in PD.

Keywords: Cerebrovascular diseases; Parkinson's disease; Pericyte; Angiogenesis; Vascular biology; Immunohistochemistry

Introduction

We have recently reported vascular degeneration in the middle frontal gyrus (MFG) of cerebral cortex, substantia nigra (SN), caudate nuclei (CN) and brainstem nuclei as part of the pathology in human Parkinson disease (PD), in which endothelial cell degeneration has been characterized as the cause of the loss of capillary networks [1]. Subsequently, we have described the changes of basement membrane which is retained and leads to an increase in string vessel formation in the PD brains [2]. Given string vessels do not carry blood, the data may suggest a potential role for hypoperfusion in secondary neuronal degeneration of PD. Apart from the CN, the maintained basement membrane may prevent the leakage of the blood-brain barrier (BBB) and the activation of astrocytes in other brain regions examined in PD [2].

The mechanism underlying endothelial degeneration is so far not clear. Vascular remodelling through angiogenesis and vascular regeneration is the key to maintain functional vascular networks. As part of the capillary structure in the central nervous system (CNS), pericytes are embedded within the basement membranes and play important roles in vascular remodelling through promoting angiogenesis, endothelial proliferation and regulating cerebral blood flow [3,4].

Several growth factors play important roles in promoting vascular remodelling. While vascular endothelial growth factor (VEGF) is essential for angiogenesis [5], insulin-like growth factor-1 (IGF-1) plays a critical role in vascular regeneration in the CNS [6]. VEGF is

broadly expressed in neurons [7], endothelial cells [8] and astrocytes [9]. Chronic hypoperfusion, for example, via increased string vessels in PD [2], can stimulate VEGF induced angiogenesis locally [8]. It is also known that VEGF stimulated angiogenesis is associated with the dysfunction of the BBB due to leakage of newly formed vessels [10]. IGF-1 is a neurotrophic factor which is also involved in vascular remodelling through regulating VEGF upstream by promoting the maturation of newly formed capillaries. IGF-1 dysfunction has been reported in neurological conditions [11]. The increase in circulating IGF-1 is used as a biomarker for IGF-1 resistance in PD [12]. The function of IGF-1 is mediated through activating its receptors which are widely distributed in different brain regions [13]. IGF-1 activity is also tightly regulated through the binding of IGF binding proteins (IGFBPs), in which IGFBP-2 is dominant in the CNS [14]. The binding to IGFBPs regulates IGF-1 function by preventing IGF-1 from being metabolised

***Corresponding author:** Jian Guan, Department of Pharmacology and Clinical Pharmacology, Faculty of Medical and Health Sciences, University of Auckland, Private Bag 92019, Auckland 1023, New Zealand, Tel: 006499236134; E-mail: j.guan@auckland.ac.nz

Received March 09, 2017; Accepted March 16, 2017; Published March 23, 2017

Citation: Yang P, Waldvogel H, Turner C, Faull R, Dragunow M, et al. (2017) Vascular Remodelling is Impaired in Parkinson Disease. J Alzheimers Dis Parkinsonism 7: 313. doi: 10.4172/2161-0460.1000313

Copyright: © 2017 Yang P, et al. This is an open-access article distributed under the terms of the Creative Commons Attribution License, which permits unrestricted use, distribution, and reproduction in any medium, provided the original author and source are credited.

and preventing IGF-1 to activate IGF-1 receptors (IGF-1R) due to higher affinity of IGF-1 to IGFBPs than to IGF-1R [15].

In order to test our hypothesis whether the impairment of capillary remodelling is associated with vascular degeneration in human PD, the current study evaluated the changes of platelet-derived growth factor receptor-beta (PDGFR β) expression in pericytes, cell proliferation of capillaries, the expression of VEGF, activation of IGF-1 receptors in capillaries and expression of IGFBP-2 in the grey matter of the where we have demonstrated both neuronal [2] and endothelial degeneration [1] in human PD.

Methods

The study has been approved by University of Auckland Human Participants Ethics Committee (Reference number 2008/279).

Tissue preparation

Tissue preparation was as previously described [16]. Briefly, the brains from the Neurological Foundation of New Zealand Human Brain Bank were perfused with 1% sodium nitrite dissolved in phosphate buffered saline (PBS) for 15 min followed by formalin fixative solution containing 15% formalin solution in 0.1 M PBS for 30-45 min. The brain samples were then placed in the same formalin fixative solution overnight. Dissection of the brain regions into blocks followed the overnight fixation process. The blocks were then embedded in paraffin.

The tissue microarray (TMA) contains the grey matter of the middle frontal gyrus (MFG) from 17 PD and 17 age-matched control cases. The production of the TMAs was based on the procedures described previously [17]. The TMA block was made using the Advanced Tissue Arrayer (VTA-100, Veridiam). Tissue cores 2 mm in diameter were extracted from the grey matter of the paraffin-embedded MFG donor blocks, and were then embedded into the cylindrical holes of matched size in an empty recipient paraffin block. The TMA block was incubated at 37°C overnight and then at 60°C for 7 min to "heal". The TMA block was cut into 7 μ m thick sections with a rotary microtome. These TMA sections were mounted onto glass slides and stored at room temperature before immunohistochemical procedures.

Case selections

The criteria for case selection has been previously described [2].

Briefly, clinically diagnosed idiopathic PD cases were donated to the Neurological Foundation of New Zealand Human Brain Bank. After tissue processing a series of several key diagnostic regions all of the PD and control cases were examined by a neuropathologist. The anatomical areas sampled included the substantia nigra, pons at the level of locus coeruleus, middle frontal gyrus, middle temporal gyrus, hippocampus with the entorhinal cortex, caudate nucleus/putamen, cingulate gyrus, inferior parietal lobule, occipital cortex and cerebellum. Tissue blocks were processed for paraffin embedding, 4 m thick tissue sections were cut, which were subsequently stained with haematoxylin and eosin, and immunohistochemistry was performed with antibodies to tau (DAKO A0024), beta-amyloid (DAKO 6F/3D) and alpha-synuclein (Leica clone KM51). Only cases consistent with idiopathic Parkinson's disease were chosen and age-matched control cases with absence of clinical neurological symptoms and only age related pathological changes in the brains were selected. All the selected cases have a post-mortem delay of less than 48 h. Information regarding the age, sex, post-mortem delay, clinical and pathological diagnosis, cause of death of PD and age-matched control cases are listed in Tables 1 and 2.

Immunohistochemical staining

The paraffin-embedded tissue microarray sections of the grey matter of the MFG were used. Immunohistochemistry was performed using antibodies labelling for pericytes, PCNA for proliferation of endothelial cells, VEGF, phosphorylated IGF-1R (IGF-1Rp) and IGFBP-2 (Table 3). The methodology has been described previously [1,16]. All washes, unless specially noted, were carried out three times for 5 minute each in PBS with gentle shaking. All antibodies were diluted with immunobuffer containing 1% donkey serum (v/v) and 0.4% merthiolate (w/v) in PBST.

The tissue microarray sections were incubated on a hotplate at 60°C for 1 hour before they were de-paraffinized in 2 changes of xylene, 10 min each. The sections were then rehydrated through a graded alcohol series consisting of 3 changes of 100% alcohol, 5 min each, 95%, 80% and 75% alcohols, 2 min each and 3 changes of water, 5 min each. Target antigens from the tissue microarrays were retrieved by heating the sections in 10mM Tris-EDTA buffer with pH10 by using a 2100 Retriever (Prestige Medical). Endogenous peroxidase was deactivated by pre-treating the sections with a solution of 50% methanol (v/v) and 1% hydrogen peroxide (v/v) for 20 min. The sections were then

Case	Age	Sex	PM delay	Pathology	Cause of Death
H215	67	F	23.5 h	No significant histological abnormalities	Ischemic Heart Disease
H204	66	M	9 h	No significant histological abnormalities	Ischemic Heart Disease
H202	83	M	14 h	No significant histological abnormalities	Ruptured abdominal aortic aneurysm
H198	67	F	27 h	No significant histological abnormalities	Ischemic Heart Disease
H196	85	M	15 h	No significant histological abnormalities	Metastatic adenocarcinoma - colon
H193	71	M	23 h	No significant histological abnormalities	Ischemic Heart Disease
H191	77	M	20 h	No significant histological abnormalities	Ischemic Heart Disease
H190	72	F	19 h	Age-related microscopic changes	Ruptured myocardial infarction
H181	78	F	20 h	No significant histological abnormalities	Aortic aneurysm
H180	73	M	33 h	No significant histological abnormalities	Ischemic Heart Disease
H169	81	M	24 h	No significant histological abnormalities	CO poisoning
H156	89	M	19 h	No significant histological abnormalities	Atherosclerosis
H154	71	M	23 h	No significant histological abnormalities	Ischemic Heart Disease
H153	76	M	8 h	Age-related changes	Ischemic Heart Disease
H152	79	M	18 h	Age-related changes	Congestive heart failure
H150	78	M	11 h	No significant histological abnormalities	Ruptured myocardial infarction
H144	76	M	18.5 h	Non-specific age-related cerebral cortical change	Ruptured aortic aneurysm

Table 1: Clinical and pathological details of control cases.

Case	Age	Sex	PM delay	Clinical diagnosis	Pathology	Cause of death
PD48	84	M	18-20 h	Idiopathic PD	SN: patchy neuronal loss with gliosis; a few LBs	Not known
PD46	77	M	34 h	Idiopathic PD	SN: Marked loss of pigmented neurons; low numbers of laminated LBs in the neuropil. LC: no LB	Pneumonia
PD42	84	M	21 h	Idiopathic PD	Moderate loss of pigmented neurons with mild gliosis.	Myocardial infarction
PD37	81	M	4 h	Idiopathic PD	SN: Moderate to marked loss of pigmented neurons, mild gliosis, pigment incontinence; occasional LBs. LC: loss of pigmented neurons and pigment incontinence; classic LBs	PD
PD33	91	M	4 h	Idiopathic PD	SN and LC: moderate neuronal loss, gliosis and poor pigmentation of some remaining neurons; classic LBs in a few neurons.	Pneumonia
PD31	67	M	25 h	Idiopathic PD	SN: Patchy loss of pigmented neurons and fibrillary gliosis. Small LBs in some residual neurons and some larger LBs in neuropil. LC: neuronal loss not obvious; a few LBs in cytoplasm	Respiratory failure
PD28	76	F	27 h	Idiopathic PD	SN not available. Some loss of pigmented neurons and LBs in LC	Pneumonia
PD27	77	M	4 h	Idiopathic PD	SN: Marked loss of pigmented neurons and gliosis; Laminated LBs in some residual neurons	End stage PD
PD23	78	F	18.5 h	Idiopathic PD	SN: Severe loss of pigmented neurons and gliosis; LBs rarely seen. Little neuronal loss and numerous LBs in LC	Pneumonia
PD21	79	F	9.5 h	Idiopathic PD	SN: Marked loss of pigmented neurons; 2 LBs. LC: less loss of pigmented neurons; many LBs.	PD
PD20	73	M	14 h	Idiopathic PD	SN: sparsely cellular and fibrillary gliosis	Congestive heart failure
PD16	79	M	8.5 h	Idiopathic PD	SN: severe loss of pigmented neurons and a commensurate degree of fibrillary astrocytosis; rare small LBs in stroma.	Pneumonia
PD14	81	M	11 h	Idiopathic PD	SN: marked loss of pigmented neurons and fibrillary gliosis; scanty eosinophilic cytoplasmic LBs in residual neurons.	Pneumonia
PD13	70	M	12 h	Idiopathic PD	SN: marked loss of pigmented neurons; laminated eosinophilic LBs in neuropil and to a lesser extent in the cytoplasm of residual pigmented neurons.	Pneumonia
PD12	76	F	3 h	Idiopathic PD	SN: Marked loss of pigmented neurons and severe fibrillary gliosis; some small intra and extra-laminated LBs	Septicaemia, myelodysplasia
PD11	69	F	36 h	Idiopathic PD	SN: marked loss of pigmented neurons; a few laminated eosinophilic LBs in residual neurons.	Perforated gastric ulcer and peritonitis
PD10	70	M	NA	Idiopathic PD	SN: mild loss of pigmented neurons; small laminated LB in a number of neurons	Pulmonary embolism

NA: Not available.

Table 2: Clinical and pathological details of PD cases.

Antibody	Source	Host	Dilution
Primary Antibodies			
PDGFR β	Cell Signalling Technology, Danvers, MA, USA	Rabbit	1:200
VEGF	Santa Cruz Biotechnology, Dallas, Texas, USA	Rabbit	1:100
IGF1Rp	Abcam, Melbourne, Australia	Rabbit	1:100
PCNA	Santa Cruz Biotechnology, Dallas, Texas, USA	Rabbit	1:100
IGFBP2	Abcam, Melbourne, Australia	Rabbit	1:100
Secondary Antibodies			
Biotinylated anti-mouse IgG	Jackson ImmunoResearch Laboratories, West Grove, PA, USA	Donkey	1:500
Biotinylated anti-rabbit IgG	Jackson ImmunoResearch Laboratories, West Grove, PA, USA	Donkey	1:500
Tertiary Antibody			
ExtrAvidin-HRP	Sigma-Aldrich Corporation, Saint Louis, MO, USA	N/A	1:1000

Table 3: List of antibodies used for DAB immunohistochemistry.

incubated in primary antibodies for 48 h at 4°C. The tissue microarrays were then washed and incubated with biotinylated secondary donkey anti-rabbit or donkey anti-mouse antibodies (1:500) for 24 h at 4°C, followed by washes and incubation with ExtrAvidin-HRP (1:1000) for 3 h at room temperature. The tissue microarrays were then washed and incubated in a DAB solution [2] for 10 to 20 min to generate a brown reaction product before the reaction was stopped by washing the sections in PBS. Sections were then dehydrated through a graded alcohol series and xylene before cover-slipping.

Image processing and analysis

The methods for image capture had been recently published [2]. Briefly, 20 images were obtained using a 20x objective lens on the Nikon E800 microscope from each “core” of the tissue microarray by automated random imaging. An image of the whole tissue microarray

section with VEGF staining was also obtained at 0.8x magnification using a Leica MZ6 modular stereomicroscope.

ImageJ

PDGFR β positive pericytes exhibited capillary-like morphology (Figures 1A and 1B). Phosphorylated IGF-1 receptors were expressed in morphologically recognised capillaries and other brain cell types. The staining of phosphorylated IGF-1 receptors in capillaries also formed a structure equivalent to capillaries seen with other markers (Figure 3A). ImageJ software (V1.46) was used to analyse the number and length of PDGFR β positive capillaries, number of vascular PCNA staining, number and length of IGF-1Rp positive capillaries, number of IGFBP-2 positive astrocytes, and density of VEGF staining in the acquired images. For PDGFR β , PCNA and IGF-1Rp staining, macros were developed in ImageJ based on previously described analysis

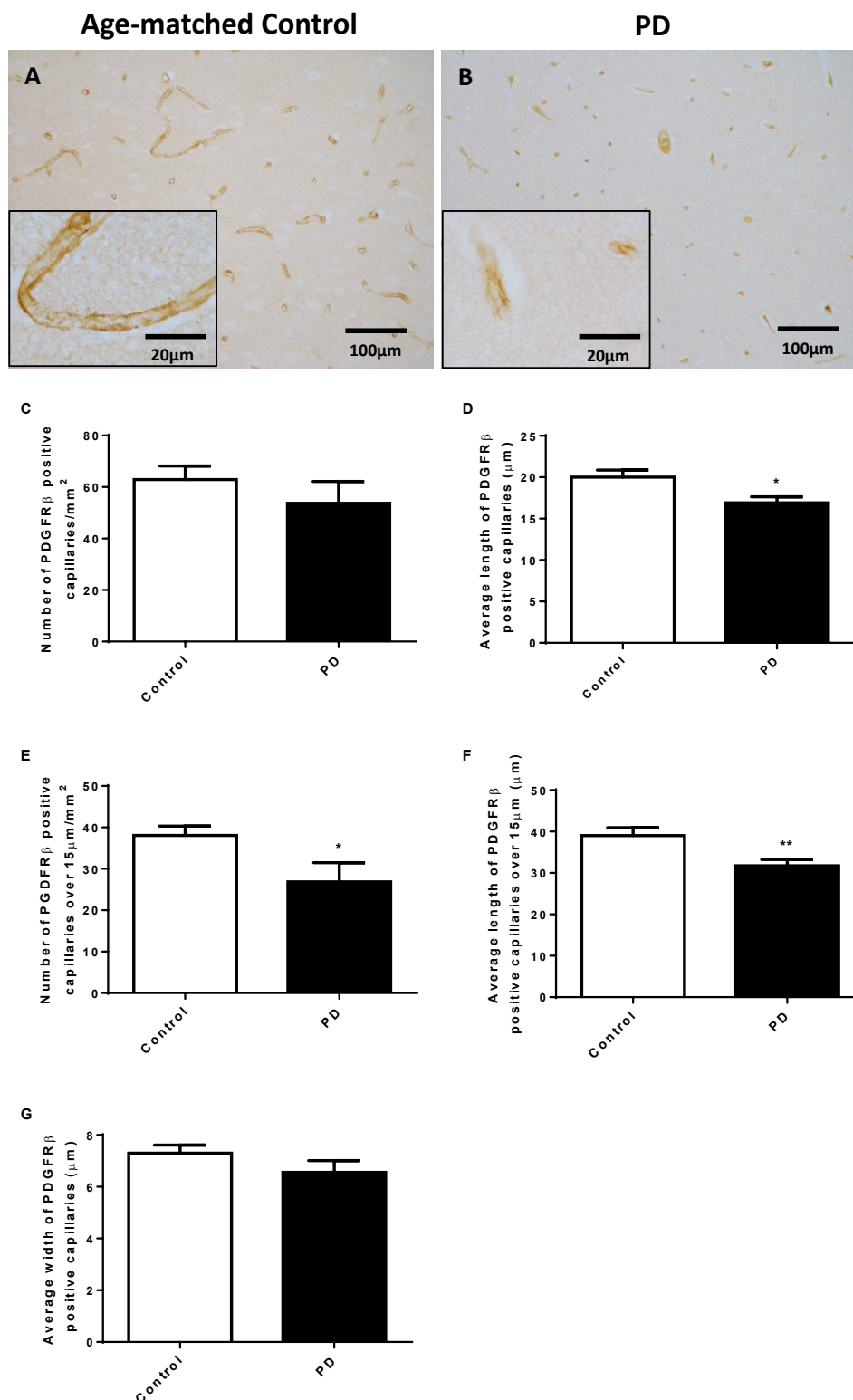


Figure 1: Shows the PDGFR β positive capillaries in the MFG of the age-matched control (A) and the PD (B) cases. PDGFR β positive pericytes show the morphology of longitudinal and cross sectional capillaries, evenly distributed in the grey matter of the MFG of both groups. PDGFR β staining was clearly located in capillary walls, which was less distinctive in the PD cases (insert C) compared with the age-matched control cases (insert D). There was no statistically significant difference between the densities (number/mm 2 , E) of PDGFR β positive capillaries of the two groups. The density (F; *p < 0.05), the total length (G; *p < 0.05) and average length (H; **p < 0.01) of the PDGFR β positive capillaries longer than 15 μ m were significantly reduced in the PD cases compared with the aged-matched control cases. There was no significant difference in average width (I) of PDGFR β positive capillaries between the two groups. MFG: middle frontal gyrus; Scale bars: 100 μ m and 20 μ m (Inserts)

methods regarding vascular staining [1] to enable automated batch processing of images. The images were first converted into 8-bit format and background was subtracted. Automatic thresholding method called “MaxEntropy” was used in the “Threshold” tool to select the targets of interest and create binary images. The “noise” of the binary images was reduced using the “Median” tool where the radius setting was 5 pixels for PDGFR β , 2 pixels for PCNA and 4 pixels for IGF-1Rp. For the analyses of PDGFR β and IGF-1Rp positive blood vessels, the “Fill Holes” tool was used to fill the enclosed hollow spaces of the vessels so that the length of the blood vessels would be measured accurately. The “Analyse Particles” tool was used to obtain the number and total length of the blood vessels. In the “Analyse Particles” tool, the shapes of the targets were filtered by setting the “circularity” range of the targets, where a circularity value of 1.0 indicates a perfect circle and a value closer to 0.0 indicates an increasingly elongated polygon. Therefore, to analyse only the blood vessels oriented longitudinally to the tissue section, non-vascular staining and cross sections of vessels were excluded from the images by setting the “circularity” option in the “Analyse Particles” tool to 0.00-0.50 for image processing. The density of blood vessels was calculated by dividing the number of vessels per image by the actual sample area of the image (0.26 mm²). The average length of the vessels in an image was acquired by dividing the total length of blood vessels by the number of vessels in the image. For vascular PCNA analysis, after the “noise” of the binary images was reduced using the “Median” tool, the “Analyse Particles” tool was used to obtain the number of vascular PCNA staining by setting “circularity” to 0.00-0.70 to include only the linear and irregular shaped staining generally found in the vessels. The density of the vascular PCNA staining was calculated by dividing the average number of vascular PCNA staining in an image by the sample area of the image (0.26 mm²). For IGFBP-2 positive astrocyte analysis, the IGFBP-2 positive astrocytes in the original images were counted using the “cell counter” tool of ImageJ, where the images were coded for blinding.

The method used for analysing the density of VEGF staining was based on the previously described intensity analysis method [2]. Briefly, the image was converted to 8 bit format before the grayscale pixel values were inverted so that stronger staining has higher pixel intensity value. Both the “cores” of the tissue microarray and a blank region of the slide were marked by using the “Freehand Selections” tool. The intensity of

the selected regions was obtained using the “Measure” tool. The pixel intensity values of the “cores” were subtracted by that of the blank region to obtain the values that represent the density of the staining on the “cores”.

Statistical analysis

The difference between the PD and age-matched control cases was analysed using two-tailed unpaired t-test. Correlation was analysed using two tailed Pearson correlation test. The r value in the correlation test represents the Pearson correlation coefficient. The data were presented as Mean \pm SEM. P value less than 0.05 was considered to be significant.

Results

Changes in pericyte associated capillaries

The photographic images in figure 1 show the expression of PDGFR β in pericytes in the MFG of an age-matched control (Figure 1A) and a PD cases (Figure 1B). The positively stained pericytes showed typical capillary structures in either longitudinal or cross section morphology. The staining was located to capillary walls where the structural images were more complete and clearer in the age-matched controls case (Figure 1, insert C) than that in the PD cases (Figure 1, insert D). Unpaired t-test analysis showed that the density (number/mm²) of pericyte associated capillaries was similar between the PD and age-matched control cases (Figure 1E). When the analysis excluded the vessels shorter than 15 μ m the density ($p < 0.05$, Figure 1F), the total length ($p < 0.05$, Figure 1G) and the average length ($p < 0.01$, Figure 1H) of the PDGFR β positive capillaries were reduced in the PD cases compared with the age-matched control cases. The average width of PDGFR β positive capillaries on the other hand, did not show a statistically significant difference between the two groups (Figure 1I).

Vascular proliferation

The photographic images in Figure 2A show PCNA positive staining, in which the darkly stained nuclei were observed in both vascular (long arrows) and non-vascular cells (arrowheads) in the MFG of both age-matched control and the PD cases. The PCNA staining in the non-vascular cells was round in shape and the staining in the vascular cells had elongated shapes. We only included the vascular

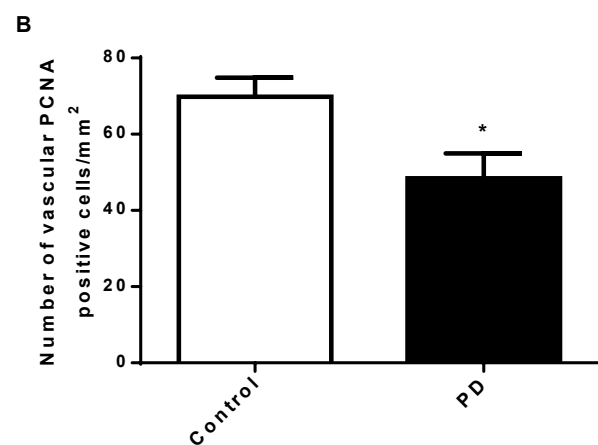
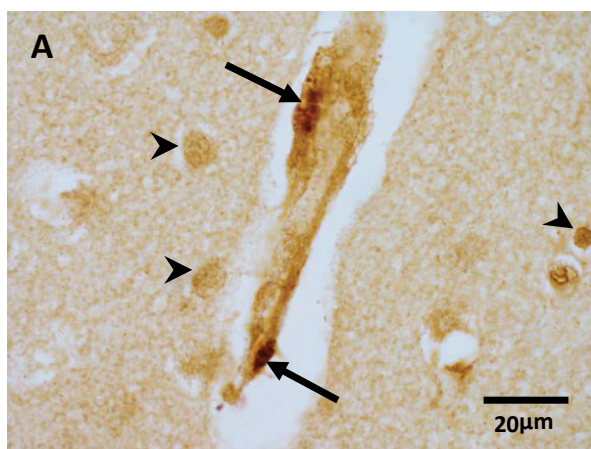


Figure 2: PCNA staining in vascular and non-vascular cells in the MFG. PCNA staining was observed in the nuclei of both vascular (A; long arrows) and non-vascular cells (A; arrowheads). Vascular PCNA staining was elongated in shapes on the blood vessel walls and was round in shape on non-vascular PCNA staining. Compared to the age-matched control cases, the number of the positive vascular PCNA staining was significantly reduced in the PD cases (B; * $p < 0.05$). MFG: middle frontal gyrus; Scale bar: 20 μ m

PCNA positive cells for quantitative analysis. Unpaired t test analysis showed that the density of vascular related PCNA positive staining evaluated as cell number/mm² in the PD cases was reduced compared with the age-matched control cases ($p < 0.05$, Figure 2B).

Phosphorylation of IGF-1 receptors in capillaries

Figure 3A shows phosphorylated IGF-1R staining in the capillary walls with both longitudinal (long arrow) and cross sectional (arrowheads) views and morphologically recognised neurons (short arrows) in the MFG of both groups. The IGF-1R staining formed a clear capillary structure where the capillaries branching off showed absence of staining. Unpaired t-test analysis showed that the density (number/mm², Figure 3B), total length (total length/mm², Figure 3C) and average length (Figure 3D) of the IGF-1Rp positive capillaries were similar between the PD and the age-matched control cases.

Pearson correlation analysis showed that the density of vascular PCNA positive cells was significantly correlated with the densities of PDGFR β positive capillaries ($r = 0.5419$, $p = 0.0011$, Figure 4A) and vascular IGF-1Rp positive cells ($r = 0.4228$, $p = 0.0142$, Figure 4B).

IGFBP-2

Figure 5 shows the distribution and morphology of IGFBP-2 positive astrocytes in the MFG of a PD case (Figures 5A and 5B). The distribution of IGFBP-2 positive astrocytes varied largely in both PD and age matched controls where IGFBP-2 positive astrocytes were broadly spread out in some cases but clustered together in other cases. There were cases from both groups showing absence of IGFBP-2 positive astrocyte. Morphologically, IGFBP-2 staining was found in both the cytoplasm and processes of the astrocytes with some of them showing clear association with blood vessels (Figure 5B). Unpaired t-test analysis showed that the density (number/mm²) of IGFBP-2 positive astrocytes was increased in the PD cases compared with the age-matched control cases ($p < 0.05$, Figure 5C).

VEGF expression

Figure 6 shows VEGF staining in the MFG (Figure 6A). VEGF expression was observed mostly in capillaries (arrowheads) and cells morphologically recognised as neurons (long arrows) and astrocytes (short arrows). Morphologically the dotted staining was clearly located around the capillaries and in the extracellular spaces (inserts). In neurons, VEGF staining was observed in cytoplasm and dendrites/

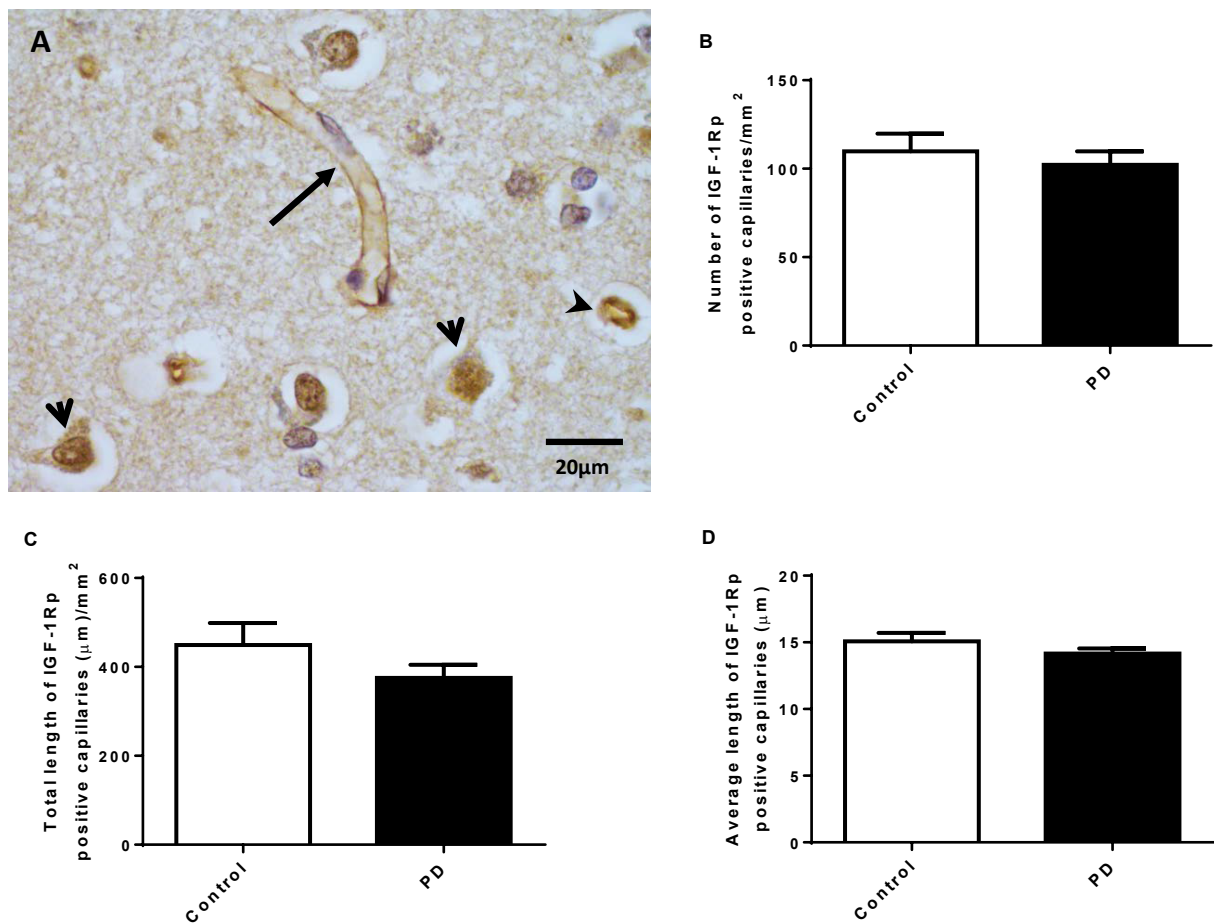


Figure 3: IGF-1Rp in capillaries and non-vascular cells in the MFG. The light micrograph showed a combination of IGF-1Rp staining (A; brown) and Nissl staining (A; purple). IGF-1Rp staining was observed in vascular walls of capillaries (A; long arrow and arrowhead) and neurons (A; short arrows). The arrow indicates an IGF-1Rp positive capillary oriented longitudinally in the section and the arrow head indicates the cross section of an IGF-1Rp positive capillary. Nissl counter staining indicated the morphology of nuclei in both vascular and non-vascular cells. There was no significant difference in the density (number/mm², B), total length (total length/mm², C) and average length (D) of IGF-1Rp positive capillaries between the PD and the age-matched control cases. MFG: middle frontal gyrus. Scale bar: 20 μm

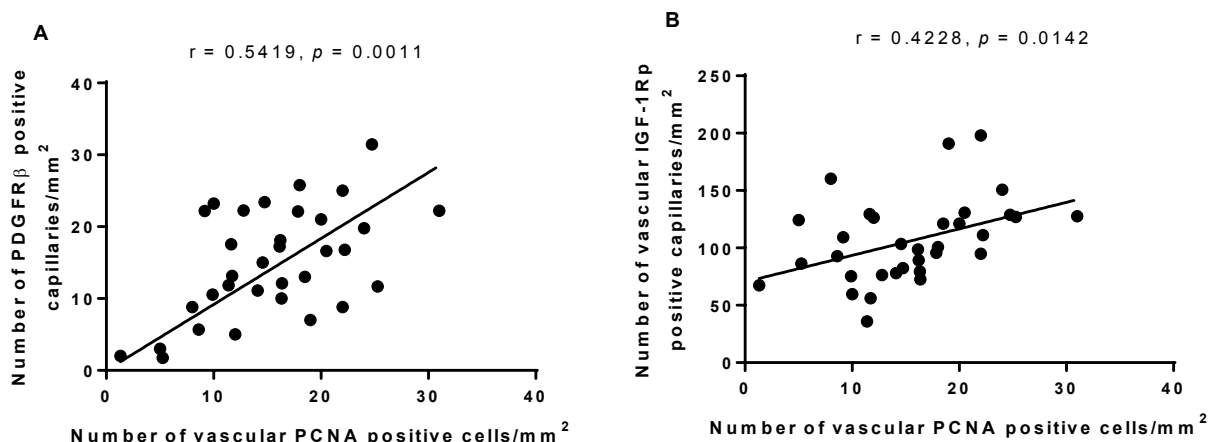


Figure 4: Correlations of vascular IGF-1R positive capillaries and PDGFR β positive capillaries with vascular PCNA staining. The density of vascular PCNA staining showed significant positive correlation with the densities of PDGFR β positive capillaries (A; $r=0.5419$, $p=0.0011$) and IGF-1R positive capillaries (B; $r=0.4228$, $p=0.0142$).

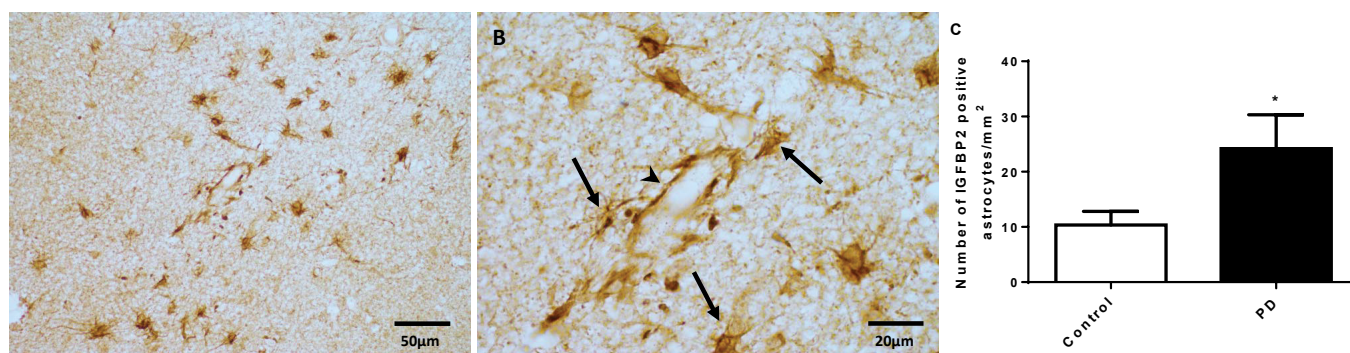


Figure 5: Shows IGFBP-2 expressing glial cells in the MFG of a PD case. IGFBP-2 staining was observed in the cytoplasm and processes of glial cells morphologically recognised as astrocytes (B; long arrows) and walls of blood vessels (B; arrowheads). In some cases, the IGFBP-2 positive astrocytes were distributed in groups (A). Some IGFBP-2 positive astrocytes were closely associated with blood vessels showing IGFBP-2 staining (B). The density of IGFBP-2 positive astrocytes in the PD cases was higher compared with the age-matched control cases (C; $*p<0.05$). MFG: middle frontal gyrus; Scale bars: 50 μ m and 20 μ m

axons (insert). The staining in astrocytes was mainly located on the processes (insert). The overall staining of the PD cases was generally lighter than that of the age matched control cases. Unpaired t-test analysis showed that the density of the VEGF staining in the PD cases was reduced compared with the age-matched control cases ($p<0.05$, Figure 6E).

Discussion

In general we found the loss of pericytes, VEGF expression and reduced vascular proliferation and in the MFG, suggesting the impaired ability in vascular remodelling of human PD brains. IGF-1 function in PD was maintained and was closely related to the loss of pericytes and vascular proliferation. The elevated IGFBP-2 in astrocytes might suggest a role for autocrine/paracrine regulation of IGF-1 in PD pathology.

The role of pericytes in vascular remodelling has been well documented [3]. As specialized mural cells, pericytes are involved in vascular remodelling by modulating endothelial cell proliferation and angiogenesis [3]. Using post mortem brain tissue from PD cases where endothelial degeneration was reported [1], we found a significant loss of pericyte-associated capillaries. Using a marker for pericytes the staining

was clearly associated with capillaries with typical tubular structure (Figures 1A-1D). By labelling the endothelial cells we have previously characterised the increase of fragmentation of the capillaries in PD [1]. Similarly while there was no statistically significant difference between the PD and control cases when the number and average width of the pericyte associated capillaries were measured (Figures 1E and 1I), we found a significant reduction in the number and length of pericyte associated capillaries when the evaluation only included the longer vessels (Figures 1F-1H). The data suggest that the loss of pericytes also involves in shorter and more fragmented capillaries, possibly due to more severe impairment in vascular remodelling. Due to tissue availability we only evaluated the changes in the MFG, in which the pericytes changes were similar to that of endothelial cells [1]. The interactions between endothelial cell and pericytes on vascular remodelling are well documented [18-20]. For example, pericytes can regulate the proliferation and survival of endothelial cells and endothelial cells mediate the recruitment of pericytes [21]. The reduced pericytes may contribute to the endothelial degeneration seen in the PD cases [1,2]. More importantly, the expression of PDGFR β was used for marking the pericytes, which is much more than just a marker of pericytes as PDGF signalling is essential for pericyte-endothelial interactions which lead to

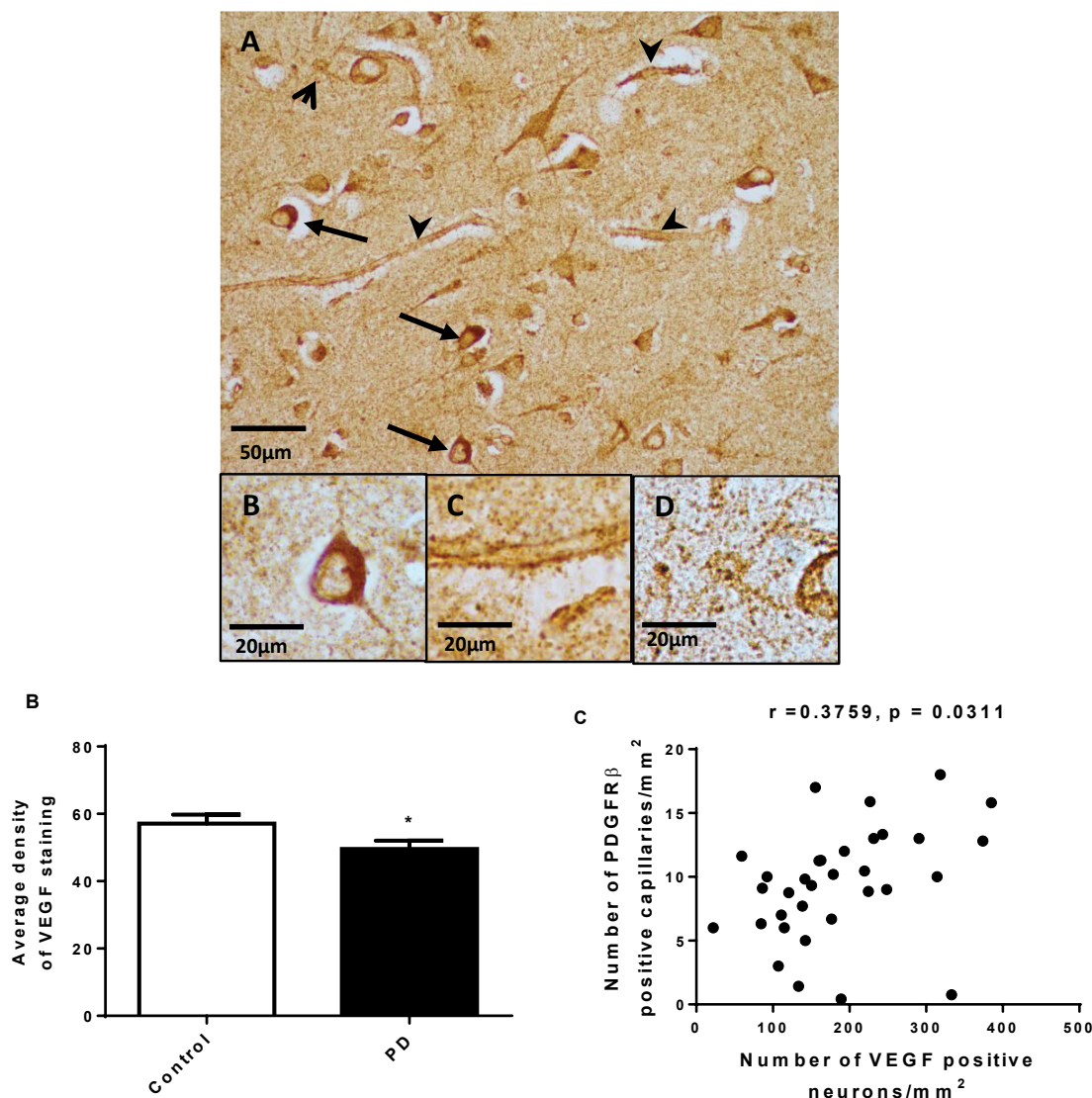


Figure 6: VEGF staining in the MFG. Positive staining was observed in neurons (A; long arrows), capillaries (A; arrowheads), astrocytes (A; short arrow) and the extracellular spaces. Punctate morphology of VEGF staining could be observed in the high resolution images (inserts B-D). In neurons, VEGF was located in the cytoplasm and the processes (insert B). In capillaries, VEGF staining was visualized along the tubular walls of the vessels (insert C). In astrocytes, VEGF staining was observed mainly on the processes (insert D). In the PD cases, the average density of VEGF staining were significantly reduced compared with the age-matched control cases in the MFG. (E; * $p < 0.05$). MFG: middle frontal gyrus; Scale bars: 50 μm and 20 μm (Inserts)

vascular remodelling through promoting vasogenesis and angiogenesis [3]. Other than PDGF receptors pericytes also express receptors for other growth factors such as VEGF receptors, transforming growth factor- β (TGF- β) receptors [21] and IGF-1 receptors [22,23]. Apart from the quantitative analysis the images of PD cases (Figures 1B and 1D) also suggested the Vascular degeneration by showing the morphology of shortened capillaries with indistinct and palely stained pericytes.

Severe loss of pericytes can lead to increased permeability of the BBB through dysfunction of endothelial cells and basement membrane deposition by astrocytes [24,25]. The reduced pericytes in PD in our study might not be severe enough to compromise the permeability of the BBB in the MFG as we have previously reported there was no increased BBB leakage and no change in basement membrane in the PD cases compared to the age matched control cases [2]. It is clear that the

preserved basement membrane prevents the leakage of large molecules; however the increase of string vessel formation due to endothelial degeneration and the remaining basement membrane may impair other functions of capillaries, such as blood supply, regulation of blood flow [26] and transport of macromolecules such as insulin, IGF-1 and low density lipoproteins from the circulation to the brain parenchyma [27].

Cell proliferation is another key mechanism of vascular remodelling. PCNA is a commonly used marker for cell proliferation, which includes endothelial proliferation. By counting the number of PCNA positive nuclei that were expressed in capillaries we also identified a decrease of cell proliferation in the capillaries. Even though we did not successfully identify the cell types that proliferate, the proliferation is likely to be associated with endothelial cells and/or pericytes due to their close associations with the capillaries (Figures 1A) [1,18,21-23].

IGF-1 deficiency has been reported in PD patients by showing increased plasma IGF-1 and IGF binding protein (IGFBP)-3 [28]. While over 75% of circulating IGFBPs are IGFBP-3 [29], the dominant binding protein in the CNS is IGFBP-2 [30]. IGFBPs regulate IGF-1 function by both inhibitory and stimulatory mechanisms [29,31]. IGF-1 has higher affinity to IGFBPs than that of IGF-1 receptors, thus the binding to IGFBPs can prevent IGF-1 activating IGF receptors, the key for initiating the downstream pathways of IGF-1 signalling [31]. Therefore, the reduction of IGFBPs could be a compensatory response to IGF-1 deficiency through increasing IGF-1 bioavailability. By evaluating the expression of IGFBP-2 in cells morphologically resembling astrocytes our study found increased IGFBP-2 in PD patients compared to the age-matched controls (Figure 5B) [32]. We do not have a clear explanation for the cause of the increase, however given the potential role for IGFBP-2 in regulating IGF-1 bioavailability in the CNS, the increased IGFBP-2 might associate with PD pathology possibly through IGF-1 resistant.

Using phosphorylated IGF-1R as an indicator for the function of IGF-1 in capillaries, we found no change in IGF-1 function between PD and control cases. A similar finding has been recently reported by another group [12], where the reduced IGF-1 receptor is only associated with Lewy bodies disease, but not PD. Given the PD cases used for current study were not Lewy body disease the changes of IGF-1 function may be the hallmark for PD with dementia [28]. Interestingly, the activation of IGF-1R was in close correlation with cell proliferation in capillaries, in which these proliferating cells were highly associated with the pericytes (Figure 4). It is known that IGF-1Rs are present in both endothelial cells [33] and pericytes [22,23]. Activation of IGF-1R in the capillaries protects capillaries from ischemic brain injury [22]. Thus the maintained IGF-1 function in PD could be a trophic response to the impaired vascular remodelling prior to development of dementia in PD. However, activation of IGF-1R may not be a specific measure for determining the presence of bioavailable IGF-1 in situations with IGF-1 function deficiency as both insulin and IGF-2 can activate IGF-1R [34], which provides compensatory pathways for insufficient IGF-1 function.

The plasma IGF-1 increases in PD patients, but reduces in PD with cognitive decline [28,35]. Although the transport of IGF-1 across the BBB is very restricted, circulating IGF-1 can directly act on IGF-1 receptors located in the luminal side of vessels to promote vascular remodelling [36]. The PD cases used for the current study were PD with no obvious cognitive impairment which may also explain the unchanged activation of IGF-1 receptors, and perhaps, maintains the BBB function through the protected basement membrane. Thus our hypothesis is that the BBB dysfunction may be an indicator for development of cognitive impairment in PD.

The effect of VEGF on neuronal survival and vascular remodelling in neurodegeneration are well documented [37-39]. Expressions of VEGF in brain tissue, particularly which in astrocytes and blood vessels are commonly used for indicating the ability in vascular remodelling. This is supported by similar reports that the VEGF was diffusely expressed on vascular walls, extracellular spaces, neurons and astrocytes [7,40-42]. By analysing the overall density of the VEGF expression, we found a general reduction of VEGF in the MFG of the PD cases. The neuronal role in vascular remodelling and the vascular role in neuronal survival through VEGF are examples of neuronal-vascular interactions [7,37]. Thus the overall expression of VEGF may provide a reliable indication of vascular remodelling [5] and therefore the decline of cerebral VEGF level may also contribute to impaired vascular remodelling and thus vascular degeneration in the PD cases. Given that IGF-1 regulates

the function of VEGF [36] the maintained IGF-1 function may be an ineffective regulatory response to the decline of VEGF.

In summary, we propose that vascular degeneration in human PD was associated with impaired vascular remodelling, possibly mediated through impaired PDGF function and the loss of pericytes. The maintained IGF-1 function was associated with vascular cell proliferation and may be an ineffective response to the loss of VEGF function. Up-regulation of IGFBP-2 may suggest a role for autocrine/paracrine regulation of IGF-1 in PD pathology.

Acknowledgement

This project was supported by the Health Research Council of New Zealand and by the Neurological Foundation of New Zealand.

References

1. Guan J, Pavlovic D, Dalkie N, Waldvogel HJ, O'Carroll SJ, et al. (2013) Vascular degeneration in Parkinson's disease. *Brain Pathol* 23: 154-164.
2. Yang P, Pavlovic D, Waldvogel H, et al. (2015) String vessel formation is increased in the brain of parkinson disease. *J Parkinsons Dis* 5: 821-836.
3. Diaz-Flores L, Gutierrez R, Madrid JF, Varela H, Valladares F, et al. (2009) Pericytes. Morphofunction, interactions and pathology in a quiescent and activated mesenchymal cell niche. *Histol Histopathol* 24: 909-969.
4. Hirschi KK, D'Amore PA (1996) Pericytes in the microvasculature. *Cardiovasc Res* 32: 687-698.
5. Breier G, Risau W (1996) The role of vascular endothelial growth factor in blood vessel formation. *Trends Cell Biol* 6: 454-456.
6. Sonntag WE, Lynch C, Thornton P, Khan A, Bennett S, et al. (2000) The effects of growth hormone and IGF-1 deficiency on cerebrovascular and brain ageing. *J Anat* 197 Pt 4: 575-585.
7. Ogunshola OO, Antic A, Donoghue MJ, Fan SY, Kim H, et al. (2002) Paracrine and autocrine functions of neuronal vascular endothelial growth factor (VEGF) in the central nervous system. *J Biol Chem* 277: 11410-11415.
8. Hai, J, Li ST, Lin Q, Pan QG, Gao F, et al. (2003) Vascular endothelial growth factor expression and angiogenesis induced by chronic cerebral hypoperfusion in rat brain. *Neurosurgery* 53: 963-970.
9. Acker T, Beck H, Plate KH (2001) Cell type specific expression of vascular endothelial growth factor and angiopoietin-1 and -2 suggests an important role of astrocytes in cerebellar vascularization. *Mechanisms of Development* 108: 45-57.
10. Nag S, Takahashi JL, Kilty DW (1997) Role of vascular endothelial growth factor in blood-brain barrier breakdown and angiogenesis in brain trauma. *J Neuropathol Exp Neurol* 56: 912-921.
11. Werner HD, Roith LE (2014) Insulin and insulin-like growth factor receptors in the brain: Physiological and pathological aspects. *Eur Neuropsychopharmacol* 24: 1947-1953.
12. Tong M, Dong M, De La Monte SM (2009) Brain insulin-like growth factor and neurotrophin resistance in parkinson's disease and dementia with lewy bodies: Potential role of manganese neurotoxicity. *J Alzheimers Dis* 16: 585-599.
13. Adem A, Jossan SS, d'Argy R, Gillberg PG, Nordberg A, et al. (1989) Insulin-like growth factor 1 (IGF-1) receptors in the human brain: quantitative autoradiographic localization. *Brain Res* 503: 299-303.
14. Guan J, Williams CE, Skinner SJ, Mallard EC, Gluckman PD (1996) The effects of insulin-like growth factor (IGF)-1, IGF-2, and des-IGF-1 on neuronal loss after hypoxic-ischemic brain injury in adult rats: Evidence for a role for IGF binding proteins. *Endocrinology* 137: 893-898.
15. Clemmons DR (1997) Insulin-like growth factor binding proteins and their role in controlling IGF actions. *Cytokine Growth Factor Rev* 8: 45-62.
16. Waldvogel HJ, Curtis MA, Baer K, Rees MI, Faull RLM (2007) Immunohistochemical staining of post-mortem adult human brain sections. *Nat Protoc* 1: 2719-2732.
17. Narayan PJ, Kim SL, Lill C, Feng S, Faull RLM, et al. (2015) Assessing fibrinogen extravasation into Alzheimer's disease brain using high-content screening of brain tissue microarrays. *J Neurosci Methods* 247: 41-49.

18. Benjamin LE, Hemo I, Keshet E (1998) A plasticity window for blood vessel remodelling is defined by pericyte coverage of the preformed endothelial network and is regulated by PDGF-B and VEGF. *Development* 125: 1591-1598.
19. Bergers G, Song S (2005) The role of pericytes in blood-vessel formation and maintenance. *Neuro Oncol* 7: 452-464.
20. ElAli A, Thériault P, Rivest S (2014) The role of pericytes in neurovascular unit remodeling in brain disorders. *Int J Mol Sci* 15: 6453-6474.
21. Ribatti D, Nico B, Crivellato E (2011) The role of pericytes in angiogenesis. *Int J Dev Biol* 55: 261-268.
22. Guan J, Gluckman P, Yang P, Krissansen G, Sun X, et al. (2014) Cyclic glycine-proline regulates IGF-1 homeostasis by altering the binding of IGFBP-3 to IGF-1. *Sci Rep* 4: 4388.
23. Sakagami K, Wu DM, Puro DG (1999) Physiology of rat retinal pericytes: Modulation of ion channel activity by serum-derived molecules. *J Physiol* 521 Pt 3: 637-650.
24. Armulik A, Genové G, Betsholtz C (2011) Pericytes: Developmental, physiological and pathological perspectives, problems and promises. *Dev Cell* 21: 193-215.
25. Armulik A, Genové G, Mäe M, Nisancioglu MH, Wallgard E, et al. (2010) Pericytes regulate the blood-brain barrier. *Nature* 468: 557-561.
26. Sumpio BE, Riley JT, Dardik A (2002) Cells in focus: Endothelial cell. *Int J Biochem Cell Biol* 34: 1508-1512.
27. Tuma PL, Hubbard AL (2003) Transcytosis: Crossing cellular barriers. *Physiol Rev* 83: 871-932.
28. Ma J, Jiang Q, Xu J, Sun Q, Qiao Y, et al. (2015) Plasma insulin-like growth factor 1 is associated with cognitive impairment in Parkinson's disease. *Dement Geriatr Cogn Disord* 39: 251-256.
29. Binoux M (1995) The IGF system in metabolism regulation. *Diabete Metab* 21: 330-337.
30. Gluckman PD, Guan J, Williams C, Scheepens A, Zhang R, et al. (1998) Asphyxial brain injury—the role of the IGF system. *Mol Cell Endocrinol* 140: 95-99.
31. Hwa V, Oh Y, Rosenfeld RG (1999) The insulin-like growth factor-binding protein (IGFBP) superfamily. *Endocr Rev* 20: 761-787.
32. Klempt ND, Klempt M, Gunn AJ, Singh K, Gluckman PD (1992) Expression of insulin-like growth factor-binding protein 2 (IGF-BP 2) following transient hypoxia-ischemia in the infant rat brain. *Brain Res Mol Brain Res* 15: 55-61.
33. Bar RS, Boes M (1984) Distinct receptors for IGF-I, IGF-II, and insulin are present on bovine capillary endothelial cells and large vessel endothelial cells. *Biochem Biophys Res Commun* 124: 203-209.
34. Adams TE, Epa VC, Garrett TPJ, Ward CW (2000) Structure and function of the type 1 insulin-like growth factor receptor. *Cell Mol Life Sci* 57: 1050-1093.
35. Pellecchia MT, Santangelo G, Picillo M, Pivonello R, Longo K, et al. (2014) Insulin-like growth factor-1 predicts cognitive functions at 2 year follow-up in early, drug-naïve Parkinson's disease. *Eur J Neurol* 21: 802-807.
36. Lopez-Lopez C, Roith D, Torres-Aleman I (2004) Insulin-like growth factor I is required for vessel modeling in the adult brain. *Proceedings of the National Academy of Sciences of the United States of America* 101: 9833-9838.
37. Wada K, Arai H, Takanashi M, Fukae J, Oizumi H, et al. (2006) Expression levels of vascular endothelial growth factor and its receptors in Parkinson's disease. *NeuroReport* 17: 705-709.
38. Ruiz de Almodovar C, Lambrechts D, Mazzone M, Carmeliet P (2009) Role and therapeutic potential of VEGF in the nervous system. *Physiol Rev* 89: 607-648.
39. Storkebaum E, Carmeliet P (2004) VEGF: A critical player in neurodegeneration. *J Clin Invest* 113: 14-18.
40. Rosenstein JM, Krum JM, Ruhrberg C (2010) VEGF in the nervous system. *Organogenesis* 6: 107-114.
41. Sá-Pereira I, Brites D, Brito MA (2012) Neurovascular unit: a focus on pericytes. *Mol Neurobiol* 45: 327-347.
42. Schiera G, Proia P, Alberti C, Mineo M, Savettieri G, et al. (2007) Neurons produce FGF2 and VEGF and secrete them at least in part by shedding extracellular vesicles. *J Cell Mol Med* 11: 1384-1394.